Organic & Biomolecular Chemistry

Accepted Manuscript

This article can be cited before page numbers have been issued, to do this please use: I. Burkhardt, N. Kreuzenbeck, C. Beemelmanns and J. Dickschat, *Org. Biomol. Chem.*, 2019, DOI: 10.1039/C8OB02744G.

ROYAL SOCIETY OF CHEMISTRY

rsc.li/obc

View Article Online
DOI: 10.1039/C8OB02744G

Organic and Biomolecular Chemistry

ARTICLE

Mechanistic Characterization of Three Sesquiterpene Synthases from the Termite-Associated Fungus *Termitomyces*

Immo Burkhardt,[a] Nina Kreuzenbeck,[b] Christine Beemelmanns[b] and Jeroen S. Dickschat*[a]

Received 00th January 20xx,
Accepted 00th January 20xx

DOI: 10.1039/x0xx00000x

www.rsc.org/

Three terpene synthases from the termite associated fungus *Termitomyces* were functionally characterized as (+)-intermedeol synthase, (–)-γ-cadinene synthase and (+)-germacrene D-4-ol synthase, with the germacrene D-4-ol synthase as the first reported enzyme that produces the (+)-enantiomer. The enzymatic mechanisms were thoroughly investigated by incubation with isotopically labeled precursors to follow the stereochemical courses of single reaction steps in catalysis. The role of putative active site residues was tested by site directed mutagenesis of a highly conserved tryptophan in all three enzymes and additional residues in (–)-γ-cadinene synthase that were identified by homology model analysis.

Introduction

With more than 80,000 members, terpenoids represent the largest class of natural products. One important step towards the structural complexity of terpenoids is the enzymatic cyclization of strikingly simple oligoprenyl pyrophosphate precursors by terpene synthases to produce (poly)cyclic terpenes, often with several stereocenters, in a single reaction.[1] These cyclizations commence by production of a carbocation that is catalyzed by the terpene synthase. In the case of type I terpene synthases, this is achieved by abstraction of pyrophosphate to yield an allylic cation.[1] Subsequently, carbon-carbon bonds are established in a cascade reaction by nucleophilic attack of double bonds from the pre-folded substrate in the enzyme's active site, which determines the regio- and stereochemical course of the reaction. Termination takes place either by final deprotonation to produce terpene hydrocarbons or by attack of a water molecule to yield terpene alcohols.[1] Investigations of these complex reactions and the interaction of the active site and the reacting substrate during catalysis has made progress using protein crystallography,[1a,2] isotopic labelling experiments[3] and theoretical investigations,[4] but to reach a more comprehensive understanding of the underlying principles of terpene cyclization reactions, more enzymes and their detailed reaction mechanisms need to be analyzed.

Higher fungi are a prolific source of bioactive terpenoid natural products like the mycotoxins T2-toxin produced by *Fusarium sporotrichioides*[5] and PR-toxin found in *Penicillium roqueforti*,[6] or the gibberellins, a group of phytohormones produced by *Fusarium fujikuroi*.[7] Most characterized fungal terpene synthases are encoded in the genomes of ascomycetes,[5-7] which comprise the largest number of known fungal species, while the second-largest group, the basidiomycetes, remains a mostly untapped source for these biosynthetic enzymes.[8] To date the only characterized type I sesquiterpene synthases from basidiomycetes originate from *Omphalotus olearius,*[9] *Stereum hirsutum,*[10] *Armillaria gallica*[11] and *Coprinus cinereus*,[12] but none of the enzymes have been investigated with respect to their cyclization mechanisms. An especially interesting taxon of basidiomycetes is the genus *Termitomyces*, whose members live exclusively in close symbiosis with fungus growing termites that actively cultivate the fungus in special chambers in their nests as foodstock.[13] The close interspecies relationship requires recognition and interaction, that is most likely mediated through volatile secondary metabolites such as terpenes.[14] Indeed, a bioinformatical analysis of the draft genome sequence of *Termitomyces* sp. J132,[15] showed the presence of 22 putative type I terpene synthase genes (STC1-STC22). None of the genes could be affiliated with a putative product, because no gene homologs had been characterized before. In the presented study we chose three of the genes for functional identification that encoded all conserved motifs, which are needed for type I terpene synthase reactivity. Two of the selected genes (STC4 and STC15) were expressed under laboratory culture conditions and could be amplified from mRNA using reverse transcriptase PCR. A third enzyme (STC9) attracted our attention, because transcriptomic studies of *Termitomyces* comb material and nodules showed high expression levels,[16] suggesting an ecological function of this enzyme and its product. The sequence of this gene with annotaded introns and exons is published in the NCBI database under accession number KNZ74377 (locus tag J132_07087) and

[a] *Kekulé-Institute of Organic Chemistry and Biochemistry, University of Bonn, Gerhard-Domagk-Straße 1, 53121 Bonn, Germany. Email: dickschat@uni-bonn.de*
[b] *Leibnitz Institute for Natural Product Research and Infection Biology, Hans-Knöll-Institute, Beutenbergstraße 11a, 07745 Jena, Germany.*

Electronic Supplementary Information (ESI) available: Procedures for cloning, enzyme expressions and purifications, in vitro experiments, product purifications and site directed mutagenesis; analytical details of identified products; additional sprectroscopical details of incubation experiments; amino acid sequences of discussed enzymes; homology model analyses for the discussed cadinene synthases; NMR spectra. See DOI: 10.1039/x0xx00000x

was obtained by gene synthesis. We report on the functional characterization of these genes *via* heterologous expression in *Escherichia coli* and purification of the corresponding enzymes, a mechanistic investigation of their cyclization mechanisms by incubation with isotopically labeled precursors and probing of different putative active site residues by site directed mutagenesis.

Results and discussion

Putative terpene synthase genes in *Termitomyces* sp. J132 were identified using antiSMASH 3.0.[17] Candidate gene sequences for STC4 and STC15 were obtained by primer-based amplification of cDNA derived from RNA isolated from the close relative *Termitomyces* sp. T153. Despite several attempts, a candidate gene sequence for STC9 could not be retrieved from mRNA of *Termitomyces* spp. and was therefore purchased via custom-based gene synthesis. All three genes were cloned into the expression vector pYE-Express[18] and heterologously expressed in *E. coli* BL21. The enzymes were purified and incubated *in vitro* with oligoprenyl diphosphate precursors. All three enzymes only converted farnesyl pyrophosphate (FPP) into sesquiterpenes or sesquiterpene alcohols, while there were no reactions with geranyl pyrophosphate (GPP), geranylgeranyl pyrophosphate (GGPP) and geranylfarnesyl pyrophosphate (GFPP). Incubations of the enzymes with FPP yielded a single product from STC9 and mixtures of sesquiterpenes from STC4 and STC15. The (main) products were purified by column chromatography in all three cases to yield a sesquiterpene alcohol from STC4, a sesquiterpene hydrocarbon from STC9 and a sesquiterpene alcohol from STC15 (for procedures, see supporting information). Their structures were unambiguously established by one and two-dimensional NMR analysis (Tables S3 – S5) and measurement of their optical rotary powers. The main product of STC4 was identified as (+)-intermedeol (**1**),[19] the single product of STC9 was (–)-γ-cadinene[20] (**2**) and the main product of STC15 was (+)-germacrene D-4-ol[21] (**3**) (Figure 1). Bacterial enzymes, which produce **1**, **2** and *ent*-**3**, but show only low sequence homology to the here identified enzymes, were characterized in our laboratories in previous studies with regard to their mechanisms.[19,20,21] To shed light on the stereochemical details of the cyclization mechanisms leading to **1**, **2** and **3** and to allow a comparison with the already described enzymes, a thorough investigation by incubation with different FPP isotopomers was carried out for each enzyme.

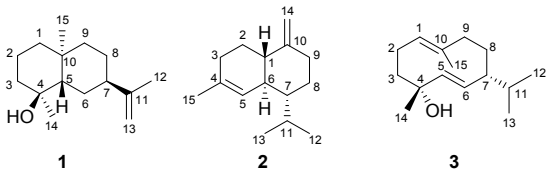

Figure 1: Main products of the terpene synthases characterized in this work.

Mechanistic characterization of STC4

The GC-MS analysis of the products obtained from an incubation experiment with FPP and STC4 showed **1** as the major enzymatic product, but α-selinene (**8**) and β-selinene (**9**) were also detected (Figure S1). Another minor compound was β-elemene, which represents the thermal Cope rearrangement product of germacrene A (**6**) and is an artifact formed in the GC-injector.[22] A possible cyclization mechanism that leads to **1** and the minor compounds starts by abstraction of pyrophosphate followed by a 1,10-cyclization to cation **5**, which after deprotonation yields germacrene A (**6**) as a neutral intermediate (Scheme 1). Reprotonation of **6** and subsequent ring closing gives rise to the cation **7**. A final attack by water yields **1**, while two alternative deprotonations of **7** can result in either **8** or **9**.

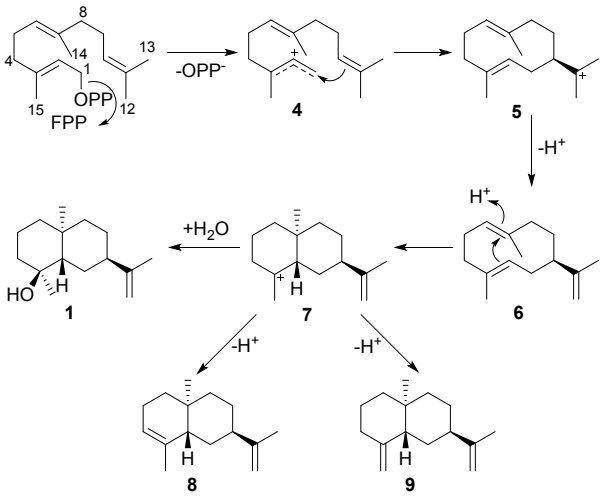

Scheme 1: Cyclization mechanism for STC4 from FPP *via* **6** towards the main product **1** and the side products **8** and **9**.

To follow the reprotonation of **6**, an incubation experiment with STC4 and (6-^{13}C)FPP in D_2O was conducted (Figure 2A). The incubation mixture was extracted with deuterated benzene and the extract was directly subjected to GC-MS and NMR analysis. An enhanced mass by +2 Da of the molecular ion of **1** in the GC-MS analysis confirmed uptake of one deuterium from D_2O to the ^{13}C-labeled compound (Figure S2). ^{13}C-NMR analysis showed a strongly enhanced triplet signal for C-1 due to ^{2}H-^{13}C ^{1}J-coupling, indicating a deuterium directly bound to the labeled carbon (Figure 2C). The stereochemical course of the reprotonation was investigated by HSQC analysis, which showed in comparison to the spectrum of unlabelled material (Figure 2D) only the crosspeak for H_α at C-1 (Figure 2E), pointing to the production of (1*S*)-(1-^{2}H,1-^{13}C)-**1**. Thus, the reprotonation takes place from the *Si*-face in **6**. The stereochemical course for the reprotonation was also addressed during the investigation of the recently characterized (+)-intermedeol synthase from *Streptomyces clavuligerus* ATCC 27064 showing the same outcome.[19] Since the amino acid sequences of both terpene synthases are not related (pairwise amino acid sequence identity of 13.9%) the results show a case of convergent evolution with regard to the product and even to the stereochemical course, in which reprotonation of intermediate **6** has to take place from the opposite face as the attack of the double bond at C-7. The regiochemistry of the deprotonation to **6** was surveyed by incubation of (12-^{13}C)FPP and (13-^{13}C)FPP

DOI: 10.1039/C8OB02744G

(Figure 3). The experiment with (12-^{13}C)FPP resulted in a product with a strongly enhanced ^{13}C signal for the C-12 methyl group in **1** (Figure 3A), while (13-^{13}C)FPP gave a product showing a strong signal for the C-13 methylene group (Figure 3B), pointing to a selective deprotonation at C-13. However, in both spectra a minor signal corresponding to the other possible position is visible (Figure 3), which suggests that also a small fraction of the deprotonation is taking place at C-12. This observation can be explained by an acting base that can reach both methyl groups next to the cationic center in 5, but the C-13 position is strongly favored.

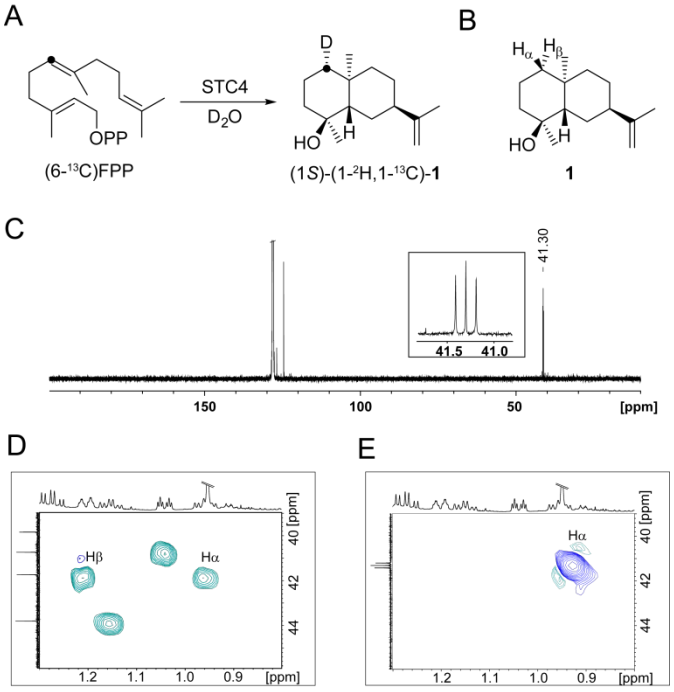

Figure 2: Incubation experiment of STC4 with (6-^{13}C)FPP. **A**: Cyclization reaction; **B**: Representation of H_α and H_β at C-1 in **1**; **C**: ^{13}C-NMR spectrum of (1-^{2}H,1-^{13}C)-**1**, showing an enhanced triplet as the signal for C-1, the signal near the solvent signal corresponds to (6-^{13}C)farnesol originating from non-enzymatic hydrolysis of (6-^{13}C)FPP; **D**: Partial HSQC spectrum of unlabeled **1**, showing cross peaks of H_α and H_β at C-1; **E**: Partial HSQC spectrum of labeled **1** from the incubation experiment, showing only the crosspeak for H_α.

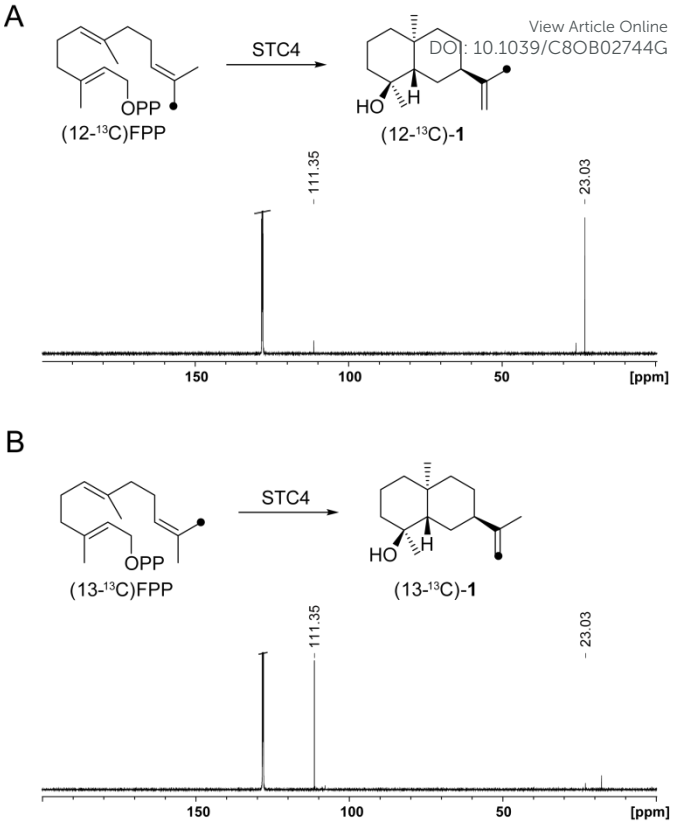

Figure 3: ^{13}C-NMR spectra resulting from the incubation experiments of STC4 with different FPP isotopomers. **A**: (12-^{13}C)FPP; **B**: (13-^{13}C)FPP.

Mechanistic characterization of STC9

GC-MS analysis of the products obtained from STC9 and FPP showed the highly selective production of γ-cadinene (**2**) (Figure S3). A possible cyclization reaction starts from FPP, which is isomerized to nerolidyl pyrophosphate (NPP) to allow a *cisoid* conformation (Scheme 2). Abstraction of pyrophosphate and a 1,10-cyclization leads to formation of the (*Z*,*E*)-germacradienyl cation **10**, that reacts by a 1,3-hydrid shift to the allylic cation **11**. Direct 1,6-ring closure leads to the cadinyl cation **12** and yields **2** after a final deprotonation.

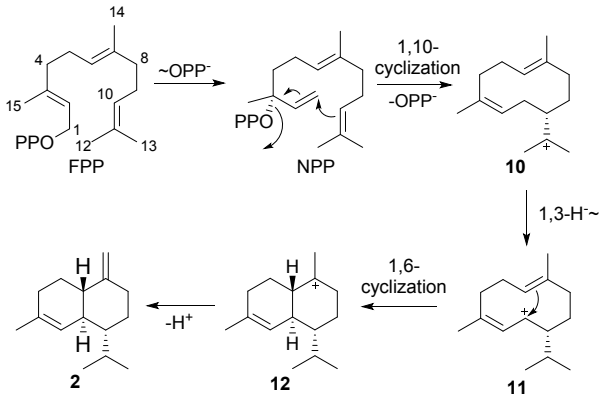

Scheme 2: Cyclization mechanism from FPP towards **2** catalyzed by STC9.

This mechanism was supported by incubation with (1,1-^{2}H$_2$,11-^{13}C)FPP to follow the 1,3-hydride shift. ^{13}C-NMR analysis of the C_6D_6 extract from the incubation showed a triplet for C-11, indicating a direct ^{2}H-^{13}C bond as expected for the proposed hydrogen migration (Figure 4A). Incubation with (1*R*)-(1-^{2}H)FPP and (1*S*)-(1-^{2}H)FPP

followed by GC-MS analysis of the products showed in both cases an increased molecular ion at *m*/*z* = 205. Moreover, the base peak of the product from (1*R*)-(1-^{2}H)FPP was detected at *m*/*z* = 162, while the product from (1*S*)-(1-^{2}H)FPP showed a base peak at *m*/*z* = 161 (Figure S4). Since the base peak corresponds to the fragment ion after cleavage of the isopropyl group (Figure S4A), the deuterium atom can be localized in the isopropyl group or within the core structure, and can thus be used to follow deuterium migration. Conclusively, the *pro-S* hydrogen at C-1 of FPP undergoes selectively the shown hydride shift. The stereochemical fate of the geminal C-12 and C-13 methyl groups in FPP was investigated by incubations with (12-^{13}C) and (13-^{13}C)FPP. Analysis of the resulting ^{13}C-NMR spectra showed that each incubation led to the selective production of only one isotopomer of **2** (Figures 4B and 4C), indicating that the 1,3-hydride migration from **10** to **11** proceeds with strict face selectivity with respect to the attack of the diastereotopic faces of the cationic center in **10**. An incubation experiment using FPP in D_2O did not produce a different isotopomer than in H_2O, as proven by GC-MS analysis, pointing to a direct cyclization mechanism as depicted in Scheme 2 and disfavoring a deprotonation-reprotonation mechanism *via* germacrene D (Scheme S1).[23]

An incubation experiment in D_2O has also been conducted for the multi-product forming cadalane synthase MtTPS5 from *Medicago truncatula*.[24] For this enzyme the formation of the neutral intermediate germacrene D and its reprotonation for further cyclization seems likely, which is also reflected by the observation of germacrene D as one of the products of the enzymatic reaction.[24] The (–)-γ-cadinene synthase from the bacterium *Chitinophaga pinensis* (Cp-γCS) was also previously studied, including mechanistic aspects with regards to the 1,3-hydride shift[21] and the stereochemical fate of the geminal methyl groups of FPP,[20] showing the same results as for STC9 in this work. Production of **2** was also shown for Omp5a and Omp5b, two terpene synthases from the basidiomycete *O. olearius*, when heterologously expressed in *E. coli*.[9] However, no information regarding the cyclization mechanism or the absolute configurations of the products was obtained in this study. STC9 shows no close sequence similarity to any of these enzymes. This represents again an example of convergent evolution.

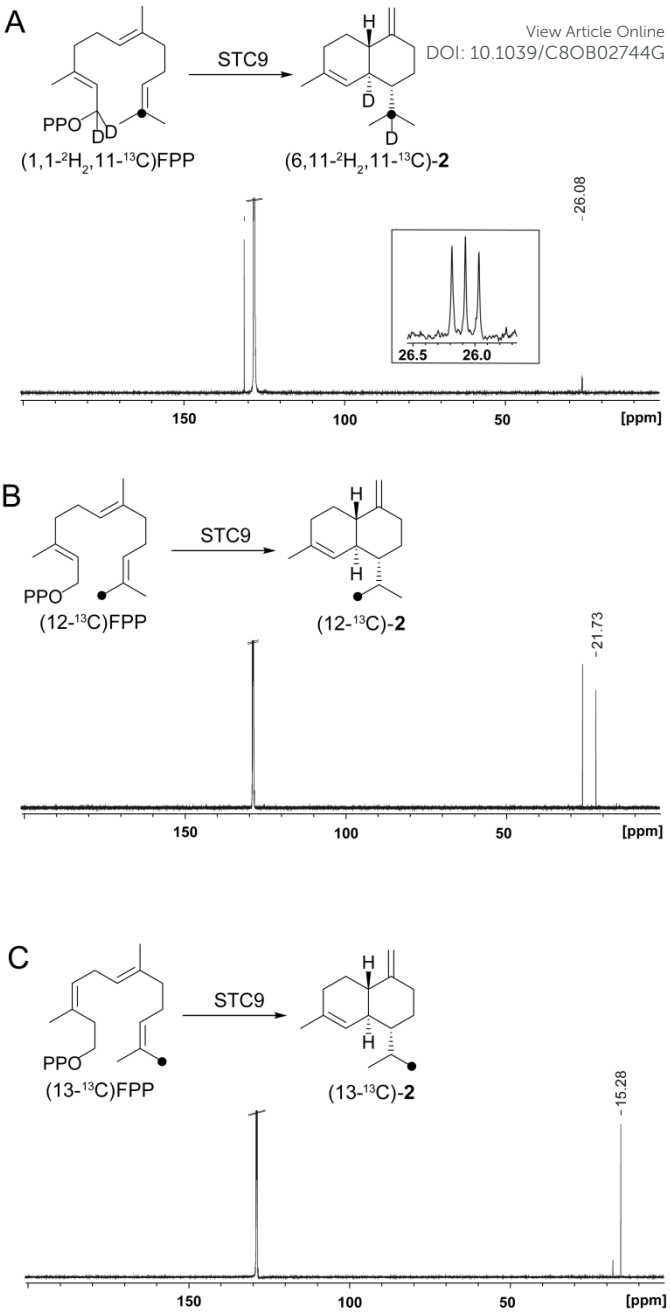

Figure 4: ^{13}C-NMR analysis of incubation experiments of STC9 using different FPP isotopomers. **A**: (1,1-^{2}H$_2$,11-^{13}C)FPP; **B**: (12-^{13}C)FPP; **C**: (13-^{13}C)FPP. Peaks not marked with chemical shifts correspond to farnesol (hydrolysed FPP).

Mechanistic characterization of STC15

Recombinant STC15 produced mainly (+)-germacrene D-(4)-ol (**3**) in *in vitro* experiments, but GC-MS analysis showed also considerable amounts of γ-cadinene (**2**), δ-cadinene (**13**), α-cadinene (**14**) and **6**, detected as its Cope rearrangement product β-elemene (**16**) (Figure S5). A cyclization mechanism that explains the formation of **3** and all cadalane-products is very similar to the STC9 mechanism, including FPP rearrangement to NPP, 1,10-ring closure, and a 1,3-hydride shift to produce intermediate **11** (Scheme 3). This allylic cation can be attacked by water, leading to production of **3**. Alternative ring closure to intermediate **12** and subsequent deprotonations yield either δ-cadinene (**13**), α-cadinene (**14**) or γ-cadinene (**2**). Notably,

View Article Online DOI: 10.1039/C8OB03746A

the formation of **6** does not require the isomerization to NPP and can proceed *via* direct 1,10-ring closure to the (*E*,*E*)-germacradienyl cation (**5**) and deprotonation.

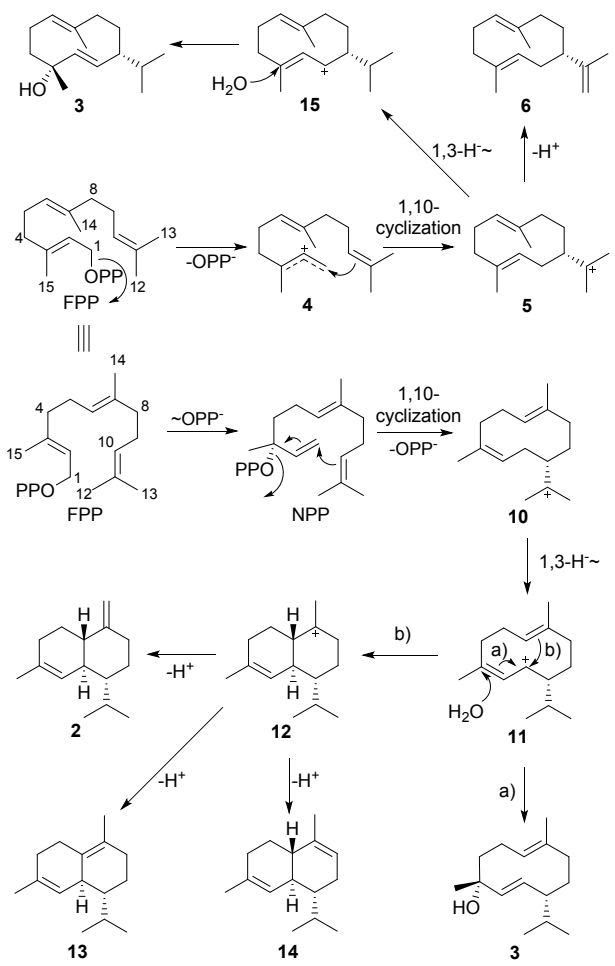

Scheme 3: Cyclization of FPP towards **3**, **2**, **13**, **14** and **6** catalyzed by STC15.

The formation of the main product **3** is also possible *via* **5**, which can undergo a 1,3-hydride shift to **15** followed by the attack of water. This mechanism was supported by incubation of (1,1-$^{2}H_2$,11-^{13}C)FPP with STC15 and subsequent NMR analysis, giving evidence for the 1,3-hydride shift by a characteristic triplet for the signal of C-11 in **3** (Figure 5A). A selective migration of the *pro-S* hydrogen in the cyclization of **3** (Figure S6) and the byproducts **2** (same result as for **2** in STC9, Figure S4), **13** (Figure S7) and **14** (Figure S8) was shown by incubation of (1*R*)-(1-^{2}H)FPP and (1*S*)-(1-^{2}H)FPP and GC-MS analysis. The stereochemical course of the hydride shift to produce **3** *via* both shown starting conformations in Scheme 3 is the same (Scheme S2), so no distinction regarding the productive starting conformation of FPP for the cyclization to **3** can be made from these experiments. A case of a mixed initial 1,10-cyclization of FPP and NPP is rare, but not unprecedented, as it was also observed for the promiscuous γ-humulene synthase from *Abies grandis*.[25] An incubation experiment in D_2O showed the same result as in H_2O and thus, as in the case of STC9, disfavors germacrene D as an uncharged intermediate that would require reprotonation (Scheme S1). The incubations of STC15 with (12-^{13}C)FPP and (13-^{13}C)FPP showed a strongly enhanced signal for only one of the geminal methyl groups of **3** (Figures 5B and 5C), pointing to a strict stereochemical course for the 1,3-hydride shift from **5**.

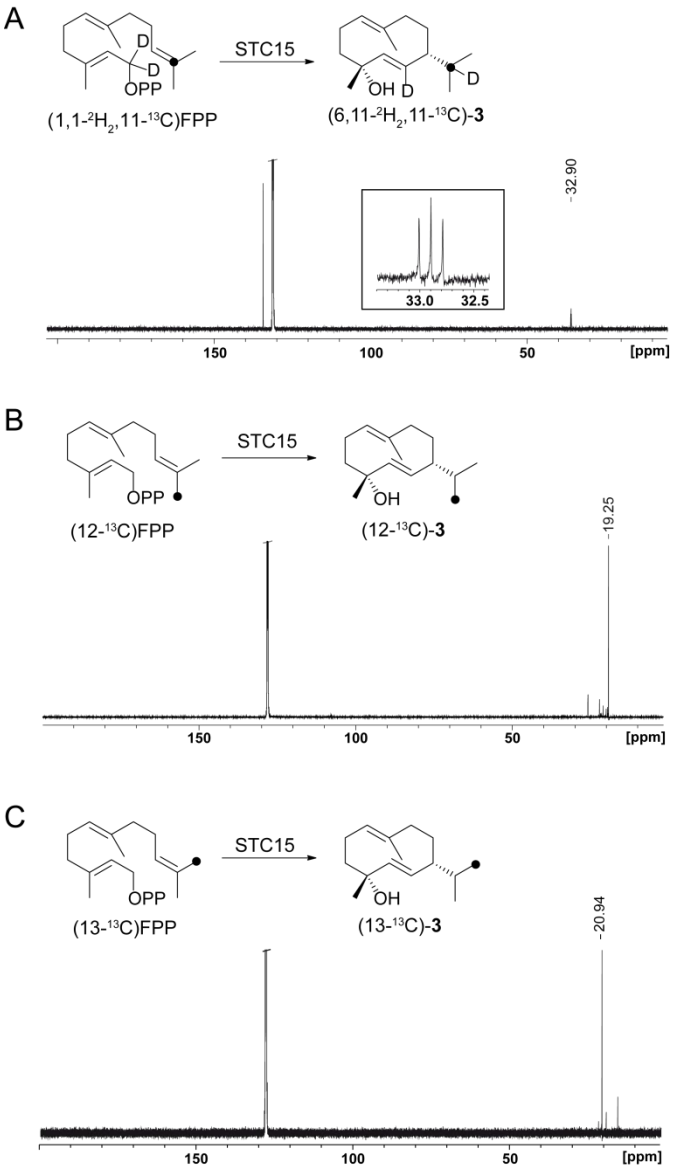

Figure 5: ^{13}C-NMR analysis of products obtained from incubation experiments of STC15 with different FPP isotopomers. **A**: (1,1-$^{2}H_2$, 11-^{13}C)FPP; **B**: (12-^{13}C)FPP; **C**: (13-^{13}C)FPP. The unmarked signal in **A** corresponds to (11-^{13}C)farnesol.

This is the first report on a germacrene D-4-ol synthase, that produces the (+)-enantiomer, while (–)-germacrene D-4-ol synthases from the bacteria *Collimonas pratensis*[21] and *Streptomyces citricolor*[26] were reported previously. Notably, the enzyme from *C. pratensis* also produces α-, δ- and γ-cadinene as side products that are, just like the main product, the enantiomers of the identified products of STC15.[21]

Site-directed mutagenesis experiments

Although type I terpene synthases often show little overall sequence similarity, there are some highly conserved motifs, like the aspartate rich motif and the NSE/DTE-triad, that are crucial for magnesium binding,[1] and the RY pair and the pyrophosphate sensor forming

hydrogen bond networks to the substrate's diphosphate.[2b] Recently, the alignment of a multitude of bacterial terpene synthase amino acid sequences revealed new conserved residues,[3c,27] most of which putatively play a major structural role for the α-domain fold. One highly conserved residue is a tryptophan, appearing six amino acid positions upstream of the RY pair. The corresponding residue was previously targeted by site directed mutagenesis experiments with pentalenene synthase[28] and with cyclooctat-9-en-7-ol synthase (CotB2).[29] For pentalenene synthase, exchange against phenylalanine did not severely affect production, but gave germacrene A (**6**) as a side product. For CotB2, the phenylalanine variant showed a decreased production of cycloocat-9-en-7-ol, while a glycine variant resulted in the formation of 3,7,18-dolabellatriene as the main product.

All three terpene synthases surveyed in this work show a tryptophan six positions upstream of RY (Figures S9-S11) and an exchange *via* site directed mutagenesis of this residue to alanine and to phenylalanine was carried out for each enzyme. In all three cases the alanine variants gave no soluble protein from heterologous expressions in *E. coli*. The effects of an exchange to phenylalanine were different in each tested enzyme. For STC4 W335F, the production of **1** was completely abolished and **6** was observed as main product, as shown by GC-MS detection of its Cope rearrangement product **16** (Figure 6). This finding suggests a strong effect of W335 on the stabilization of cation **7** by cation-π-interactions that may be important for downstream reactions from **6** (Scheme 1). Such a stabilization is less pronounced for phenylalanine.[30] However, **7** and **8** are still observed in the W335F variant. A possible explanation is that these compounds are formed non-enzymatically from **6**, a reaction that smoothly proceeds by mild acid catalysis in solution or on silica gel.[31] The STC9 W314F variant showed the same product specificity and the same activity (Figure 7) as the wild type enzyme, so W314 can be substituted by Phe for efficient catalysis by this enzyme. In the case of STC15, the heterologous expression of the W314F variant failed to produce soluble protein.

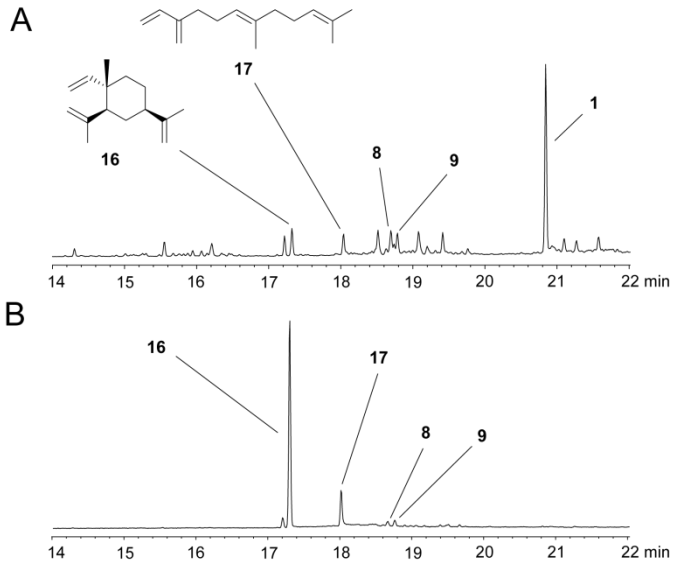

Figure 6: GC-MS analysis of incubations of STC4 incubations using FPP. **A**: wild type; **B**: W335F variant. Compound **17** is a non-enzymatic degradation product of FPP and also occurs without enzyme.

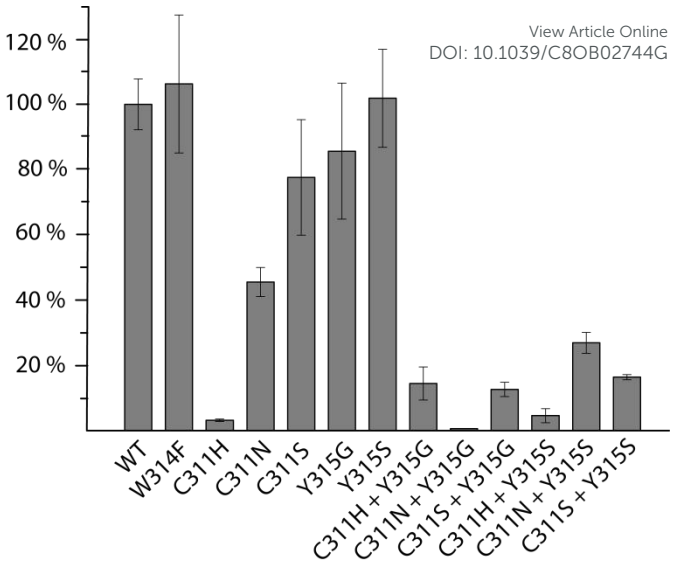

Figure 7: Relative amount of produced **2** of STC 9 (set to 100%) and its tested variants as determined by comparative incubations followed by GC-MS analysis. All experiments were carried out in triplicate.

Since Cp-γCS produced the same enantiomer of (–)-**2** via the same cyclization mechanism as STC9, homology models of both enzymes based on the crystal structure of selinadiene synthase from *Streptomyces pristinaespiralis* (PDB code 4OKM, SdS)[2b] were constructed and compared to a homology model of the (–)-δ-cadinene synthase from *S. clavuligerus* (Sc-δCS),[32] based on the same crystal structure (Figures S12 – S15). (–)-δ-Cadinene (**13**) produced by Sc-δCS exhibits an absolute configuration corresponding to the absolute configuration of **2** and its cyclization was also shown to proceed *via* a 1,3-hydride shift of the *pro-S* proton.[32] Only the last deprotonation step to produce **13** is different (Scheme 3) and thus polar residues from the three synthases that point into the active site and could interfer with the mode of deprotonation were compared. The most promising residues were C311 and Y315 in STC9, which are positioned next to the conserved W314 (Figures S10 and S12). The corresponding positions are occupied by Asn and Ser in Cp-γCS (Figure S13) and by His and Gly in Sc-δCS (Figure S14). While there are two polar residues, that can provide hydrogen bonds in the two γ-cadinene synthases, a basic residue and a glycine occur in Sc-δCS, the first of which could account for the alternative deprotonation of cationic intermediate **12** towards **13** instead of **2**. Variants of STC9 with exchange of a single residue were constructed (C311H, C311N and C311S, and Y315G and Y315S). The product spectrum of all variants was unchanged, still showing selective production of **2**, but the production was strongly decreased in the C311H variant (3%) and moderately affected in the C311N variant (45%) (Figure 7). For the C311S, Y315G and Y315S variants the production was comparable to WT STC9. When the Y315 and C311 mutations were combined in one enzyme variant, compound **2** was still the only detectable product, but the relative enzyme activity dropped significantly, ranging from 1% production by the C311N/Y315G variant to 30% by the C311N/Y315S variant. These mutagenesis experiments show the dependency of efficient catalysis by STC9 on C311, only exchange with its oxygen analog Ser retained almost the same productivity (80%) than in the WT enzyme. Y315 exchange does not seem to be

critical, but when it was exchanged by Gly or Ser in combination with C311 mutations the productivity dropped more severely in all tested cases. Since both original residues C311 and Y315 are rather hydrophobic,[33] replacement by more hydrophilic residues may disturb the hydrophobic cavity and thus hamper catalysis, but detailed insights into the particular roles of these residues will require structural data of STC9.

Conclusions

We characterized three terpene synthases from the termite associated fungus *Termitomyces*, an interesting species with largely untapped secondary metabolism, as (+)-intermedeol synthase (STC4), (–)-γ-cadinene synthase (STC9) and (+)-germacrene D-4-ol synthase (STC15). Two of the enzymes were expressed under standard laboratory culture conditions (STC4 and STC15), while the third enzyme (STC9) was found to be strongly expressed in *Termitomyces* comb material and nodules, but not in laboratory cultures, which may point to an ecological function. The cyclization reactions were surveyed for all three enzymes using incubations with isotopomers of FPP, shedding light on the stereochemical courses of ring closing and reprotonation steps, and hydride shifts during catalysis. Terpene synthases, responsible for the production of **1** and **2**, that are not sequentially related to the investigated enzymes from this work, were mechanistically characterized before and showed the same reaction courses as determined here. STC15 represents the first characterized (+)-germacrene D-4-ol synthase, yet, the enantiomers of the side products **2**, **13** and **14** were produced by germacrene D-4-ol synthase from *C. pratensis*,[21] showing a mirrored chemistry with respect to STC15. The role of a highly conserved tryptophan in type-I terpene synthases for catalysis was probed, showing high importance in the cyclization of STC4, which turned to a selective germacrene A synthase after a single W335F mutation. The same point mutation had no effect on catalysis in STC9, while no protein could be obtained for W314 variants of STC15. The putative active site residue C311 in STC9 was mutated, leading to variants with decreased productivity, but no change of the main product **2**. The effect was even stronger in combination with Y315 exchange, which alone showed no effect.

This study clearly shows convergent evolution of terpene synthases in very distantly related organisms, promoting the same terpene cyclization cascades likely by forcing the FPP precursor into a similar reactive conformation in the enzymes' active sites, and then taking advantage of the resulting intrinsic reactivity just triggered by pyrophosphate abstraction.[23,34] The particular roles of the active site residues, that are responsible for positioning of the substrate is still puzzling as also shown by the diverse effects of site directed mutagenesis experiments in this work. For possible future pattern recognition in sequences of terpene synthases, which hint towards the carried out mechanism of the enzyme, more of these enzymes need to be characterized and analyzed with regard to mechanistic details and the role of ensembles of active site- and structure determining residues. This ongoing endeavor will be continued by future studies in our laboratories. We will also address the interesting question of the ecological role of terpenes in the interactions between Termitomyces and its associated termites.

Conflicts of interest

There are no conflicts to declare.

View Article Online
DOI: 10.1039/C8OB02744G

Acknowledgements

This work was supported by the DFG with grant DI1536/9-1 and the CRC 1127 ChemBioSys. We thank M. T. Poulsen (University of Copenhagen, Denmark) and Z. W. de Beer (FABI, University of Pretoria) for supporting our field work.

References

1 (*a*) J. S. Dickschat, *Nat. Prod. Rep.*, 2016, **33**, 87-110; (*b*) D. W. Christianson, *Chem. Rev.*, 2017, **117**, 11570-11648; (*c*) J. S. Dickschat, *Nat. Prod. Rep.*, 2011, **28**, 1917-1936; (*d*) D. J. Miller and R. K. Allemann, *Nat. Prod. Rep.*, 2012, **29**, 60-71.

2 (*a*) M. J. Rynkiewicz, D. E. Cane and D. W. Christianson, *Proc. Natl. Acad. Sci. USA*, 2001, **98**, 13534-13548; (*b*) P. Baer, P. Rabe, K. Fischer, C. A. Citron, T. A. Klapschinski, M. Groll and J. S. Dickschat, *Angew. Chem. Int. Ed.*, 2014, **53**, 7652-7656; (*c*) J. M. Caruthers, I. Kang, M. J. Rynkiewicz, D. E. Cane and D. W. Christianson, *J. Biol. Chem.*, 2000, **275**, 25533-25539.

3 (*a*) J. S. Dickschat, *Eur. J. Org. Chem.*, 2017, 4872-4882; (*b*) C.-M. Wang, R. Hopson, X. Lin and D. E. Cane, *J. Am. Chem. Soc.*, 2009, **131**, 8360-8361; (*c*) L. Lauterbach, J. Rinkel and J. S. Dickschat, *Angew. Chem. Int. Ed.*, 2018, **57**, 8280-8283; (*d*) A. Meguro, Y. Motoyoshi, K. Teramoto, S. Ueda, Y. Totsuka, Y. Ando, T. Tomita, S.-Y. Kim, T. Kimura, M. Igarashi, R. Sawa, T. Shinada, M. Nishiyama and T. Kuzuyama, *Angew. Chem. Int. Ed.*, 2015, **54**, 4353-4356; (*e*) B. Qin, Y. Matsuda, T. Mori, M. Okada, Z. Quan, T. Mitsuhashi, T. Wakimoto and I. Abe, *Angew. Chem. Int. Ed.*, 2016, **55**, 1658-1661.

4 (*a*) D. J. Tantillo, *Nat. Prod. Rep.*, 2011, **28**, 1035-1053; (*b*), D. T. Major, Y. Freud and M. Weitman, *Curr. Opin. Chem. Biol.*, 2014, **21**, 25-33; (*c*) M. Dixit, M. Weitman, J. Gao and D. T. Major, *ACS Catal.*, 2017, **7**, 812-818.

5 A. E. Desjardins, *J. Agric. Food Chem.*, 2009, **57**, 4478-4484.

6 R. Riclea and J. S. Dickschat, *Angew. Chem. Int. Ed.*, 2015, **54**, 12167-12170.

7 C. Böhmke and B. Tudzynski, *Phytochemistry*, 2009, **70**, 1876-1893.

8 C. Schmidt-Dannert, *Adv. Biochem. Eng. Biotechnol.*, 2015, **148**, 19-61.

9 G. T. Wawrzyn, M. B. Quin, S. Choudhary, F. Lopez-Gallego and C. Schmidt-Dannert, *Chem. Biol.*, 2012, **19**, 772-783.

10 (*a*) C. M. Flynn and C. Schmidt-Dannert, *Appl. Environ. Microbiol.*, 2018, **84**, e00036-18; (*b*) M. B. Quin, C. M. Flynn, G. T. Wawrzyn, S. Choudhary and C. Schmidt-Dannert, *ChemBioChem*, 2013, **14**, 2480-2491.

11 B. Engels, U. Heinig, T. Grothe, M. Stadler and S. Jennewein, *J. Biol. Chem.*, 2011, **286**, 6871-6878.

12 S. Agger, F. Lopez-Gallego and C. Schmidt-Dannert, *Mol. Microbiol.*, 2009, **72**, 1181-1195.

13 (*a*) H. H. de Fine Licht, J. J. Boomsma and D. K. Aanen, *Mol. Ecol.*, 2006, **15**, 3131-3138; (*b*) C. Beemelmanns, H. Guo, M. Rischer and M. Poulsen, *Beilstein J. Org. Chem.*, 2016, **12**, 314-327.

14 (*a*) H.-P. Li, W.-J. Yang, S.-X. Qu, F. Pei, X. Luo, A. M. Mariga and L. Ma, *Food Res. Int.*, 2018, **103**, 150-155; (*b*) J. S. Dickschat, *Nat. Prod. Rep.*, 2017, **34**, 310-328; (c) F. A. Ditengou, A. Müller, M. Rosenkranz, J. Felten, H. Lasok, M. M. van Doorn, V. Legué, K. Palme, J.-P. Schnitzler and A. Polle, *Nat. Commun.*, 2015, **6**, 6279.

15 M. Poulsen, H. Hu, C. Li, Z. Chen, L. Xu, S. Otani, S. Nygaard, T. Nobre, S. Klaubauf, P. M. Schindler, F. Hauser, H. Pan, Z. Yang,

A. S. M. Sonnenberg, Z. W. de Beer, Y. Zhang, M. J. Wingfield, C. J. P. Grimmelikhuijzen, R. P. de Vries, J. Korb, D. K. Aanen, J. Wang, J. J. Boomsma and G. Zhang, *Proc. Natl. Acad. Sci. USA*, 2014, **111**, 14500-14505.
16 H. Hu, PhD Dissertation, Copenhagen, 2019.
17 T. Weber, K. Blin, S. Duddela, D. Krug, H. U. Kim, R. Bruccoleri, S. Y. Lee, M. A. Fischbach, R. Müller, W. Wohlleben, R. Breitling, E. Takano and M. H. Medema, *Nucl. Acids Res*., 2015, **43**, W1, W237-W243.
18 J. S. Dickschat, K. A. K. Pahirulzaman, P. Rabe and T. A. Klapschinski, *ChemBioChem*, 2014, **15**, 810-814.
19 P. Rabe, J. Rinkel, T. A. Klapschinski, L. Barra and J. S. Dickschat, *Org. Biomol. Chem*., 2016, **14**, 158-164.
20 P. Rabe, T. Schmitz and J. S. Dickschat, *Beilstein J. Org. Chem.*, 2016, **12**, 1839-1850.
21 J. Rinkel, P. Rabe, P. Garbeva and J. S. Dickschat, *Angew. Chem. Int. Ed*., 2016, **55**, 13593-13596.
22 A. M. Adio, *Tetrahedron*, 2009, **65**, 5145-5159.
23 D. Arigoni, *Pure Appl. Chem*., 1975, **41**, 219-245.
24 S. Garms, T. G. Köllner and W. Boland, *J. Org. Chem*., 2010, **75**, 5590-5600.
25 Y. Yoshikuni, T. E. Ferrin and J. D. Keasling, *Nature*, 2006, **440**, 1078-1082.
26 C. Nakano, F. Kudo, T. Eguchi and Y. Ohnishi, *ChemBioChem*, 2011, **12**, 2271-2275.
27 J. Rinkel, L. Lauterbach and J. S. Dickschat, *Angew. Chem. Int. Ed.*, 2017, **56**, 16385-16389.
28 (*a*) M. Seemann, G. Zhai, J.-W. de Kraker, C. M. Paschall, D. W. Christianson and D. E. Cane, *J. Am. Chem. Soc.*, 2002, **124**, 7681-7689; (b) D. E. Cane and Q. Xue, *J. Am. Chem. Soc*., 1996, **118**, 1563-1564.
29 (*a*) R. Driller, S. Janke, M. Fuchs, E. Warner, A. R. Mhashal, D. T. Major, M. Christmann, T. Brück and B. Loll, *Nat. Commun*., 2018, **9**, 3971; (*b*) R. Janke, C. Görner, M. Hirte, T. Brück and B. Loll, *Acta Crystallogr. D Biol. Crystallogr*., 2014, **70**, 1528-1537.
30 (*a*) D. A. Dougherty, *Science*, 1996, **271**, 163-168; (*b*) J. P. Gallivan and D. A. Dougherty, *Proc. Natl. Acad. Sci. USA*, 1999, **96**, 9459-9464.
31 (*a*) J. A. Faraldos, Y. Zhao, P. E. O'Maille, J. P. Noel and R. M. Coates, *ChemBioChem*, 2007, **8**, 1826-1833; (*b*) A. M. Adio, C. Paul, H. Tesso, P. Kloth and W. A. König, *Tetrahedron Asym.*, 2004, **15**, 1631-1635; (c) J.-W. de Kraker, M. C. R. Franssen, A. de Groot, W. A. König and H. J. Bouwmeester, *Plant Physiol.*, 1998, **117**, 1381-1392.
32 Y. Hu, W. K. W. Chou, R. Hopson and D. E. Cane, *Chem. Biol*., 2011, **18**, 32-37.
33 N. Nagano, M. Ota and K. Nishikawa, *FEBS Lett*., 1999, **458**, 69-71.
34 D. J. Tantillo, *Angew. Chem. Int. Ed*., 2017, **56**, 10040-10045.

Table of contents graphic:

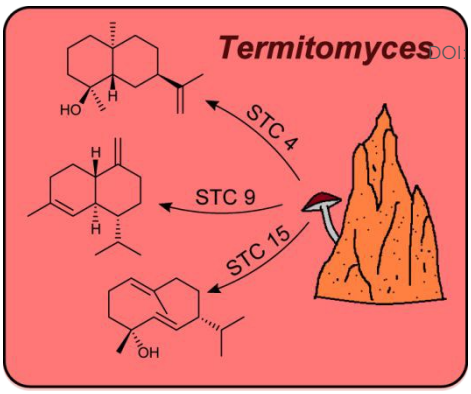

View Article Online
DOI: 10.1039/C8OB02744G

Text for Table of contents:

Three terpene synthases from the termite associated fungus *Termitomyces* were studied by isotopic labelling experiments and site-directed mutagenesis.